Unbalance compensation topology for railway application based on pulse width modulation alternating current chopper

Ismail Mir[1], Anas Benslimane[1], Jamal Bouchnaif[2], Badreddine Lahfaoui[2]
[1]Laboratory Renewable Energy, Embedded System, and Information Processing, National School of Applied Sciences,
University of Mohammed I, Oujda, Morocco
[2]Laboratory of Electrical Engineering and Maintenance, Higher School of Technology, University of Mohammed I, Oujda, Morocco

Article Info

ABSTRACT

This paper focuses the study on the design of a new topology of unbalance compensators adopted by railway operators in the substations of high-speed railway lines, this compensation structure based on the concept of alternating current (AC)-chopper controlled impedance (CCI). The present document describes the CCI compensator in terms of the components constituting this structure, the installation of CCI to limit the unbalance factor according to the limit imposed by the moroccan energy provider (ONEE), and the calculation of the power losses generated by the CCI and the comparison with other topologies such as voltage source inverter STATCOM (VSI) and current source inverter STATCOM (CSI). The modelization of the compensator and the results were established using MATLAB/Simulink software by exploiting real data provided by the moroccan railway office (ONCF).
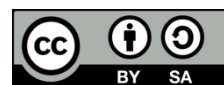
Corresponding Author:

Ismail Mir
Laboratory Renewable Energy, Embedded System, and Information Processing
National School of Applied Sciences, University of Mohammed I
Oujda, Morocco
Email: ismail.mir@ump.ac.ma

1. INTRODUCTION

Since the year 1981, high-speed railway is supplied by two-phase system 2×25 kV between the catenary and a complementary cable called negative feeder, a 25 kV between the catenary and the rail is obtained by a mid-point autotransformer as shown in Figure 1 [1], [2]. An electrical system is balanced if, for the three-phase quantities (current and voltage), it has the same amplitude, the same frequency, and a phase shift of 120°, otherwise, the system is unbalanced. The fact that the railway substations are two-phase loads with a very high dynamic power consumption, is an important source of unbalance. Therefore, it will affect the quality of the power supply by increasing the losses of the generator, reducing the output capacity of the transformer, disturbing the protective relays, devices that generate operating errors. These negative effects seriously influence the operational safety of the electrical system [3]-[5].

The orientation towards the use of compensators in railway lines has become mandatory to avoid the degradation of the electrical power quality. For this reason, the research in this field is interested in studying the compensator topologies citing the first one is the voltage source inverter STATCOM (VSI), which is based on the use of a number of compensation cells coupled in parallel to the secondary of a three-phase transformer connected by Yy0; each cell contains a filtering inductance on the alternating current (AC) side (L), a voltage source inverter with a sine-triangle pulsewidth modulation (PWM) control and a voltage storage source on the direct current (DC) side consisting of a capacitor (CDC) [6]-[9], Figure 2 illustrates the

general structure of the compensator VSI. The second one is the current source inverter STATCOM (CSI), it is composed of several cells coupled in parallel with the secondary of the three-phase transformer with a Yy0 connection. Each cell contains a DC source realized by an inductor Ldc, a CSI converter composed of six unidirectional power electronic switches (only insulated gate bipolar transistor (IGBT)), and an LC filter connected between the AC side of the inverter and the secondary of the transformer, the IGBT switches are controlled by PWM signals [10]-[14], Figure 3 illustrates the general structure of the compensator CSI.

The efficiency of the CSI compensator is higher than that of the VSI compensator in terms of power losses in the semiconductors, but the inconvenience of the CSI compensator is the complexity of the protection devices due to the current source. For this reason, this paper presents a new topology of unbalance compensation based on AC-chopper controlled impedance concept (CCI), with a classical adjustment of the protection devices and a high efficiency in terms of power losses in the semiconductors. In order to evaluate the efficiency of the CCI compensator, it has been introduced in the two sub-stations Tangier and Kenitra.

The rest of this paper are organized as follow: Section 2 describes the technical characteristics of the two substations (Tangier and Kenitra). It also presents the unbalance factor without the use of a compensator. Section 3 describes the new compensator topology and the sizing of the compensator constitution. Section 4 discusses the results obtained by the CCI compensator for the two substations on the one side, on the other side a comparison in terms of power losses between the CCI compensator and the other compensators (VSI and CSI). Section 5 concludes the paper.
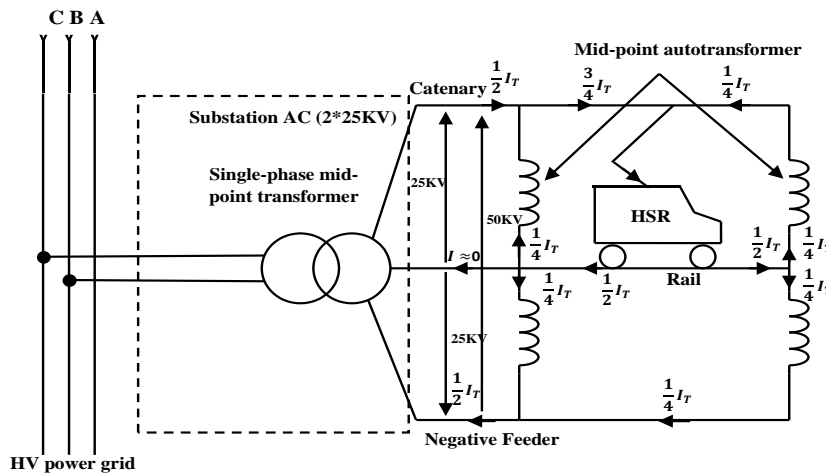

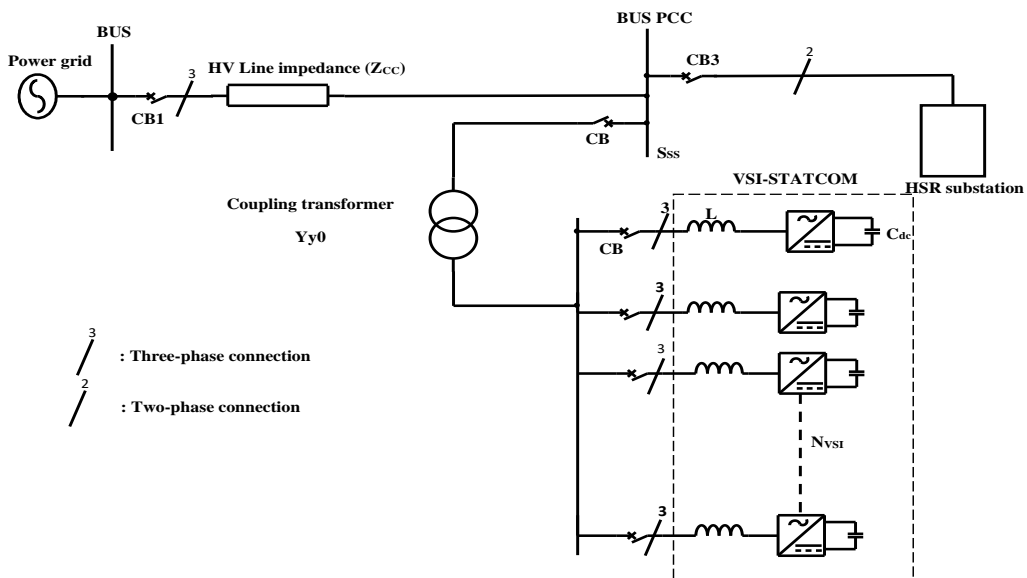Figure 1. The power circuit of supply AC system (2×25 kV -50 Hz) of the HSR substation
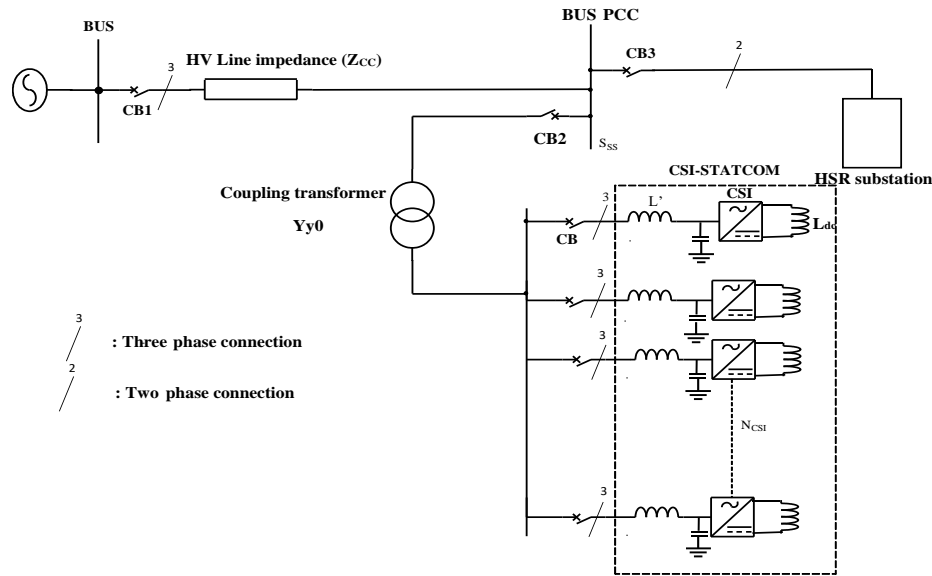

Figure 2. VSI-STATCOM structure

Figure 3. CSI-STATCOM structure

2. UNBALANCE ANALYSIS

The technical characteristics of the two Moroccan substations (Tangier and Kenitra) and the high voltage (HV) lines for the 2030 horizon are presented in Table 1 [1]. The data provided by the ONCF of the two sub-stations are spread over 9 hours from 7am to 4pm. At the point of common coupling (PCC) without compensator, based on the simulation in MATLAB/Simulink simpowersys environment. Figure 4 presents the evolution of different parameters (power consumed and unbalance factor) in normal situation (N) for Tangier substation, Figure 4(a) presents the power consumed, and Figure 4(b) presents the results of the voltage unbalance analysis.

Table 1. Characteristics of the Kenitra and Tangier substations

| Characteristics		Tangier-side substation (PK10)	Kenitra-side substation (PK185)
Rated power of the single-phase transformer		40 MVA	40 MVA
Connection		Two-phase	Two-phase
Rated voltage of the line HT		225 kV	225 kV
Short-circuit power at the Connection Point (PCC) in MVA	N: normal power grid situation(225 kV)	2800	3000
	N-1: degraded power grid situation (202 kV)	2390	2400
Line parameters		Rline (Ω/Km)=0.07	Rline (Ω/Km)=0.07
		Lline (mH/Km)=1.26	Lline (mH/Km)=1.26
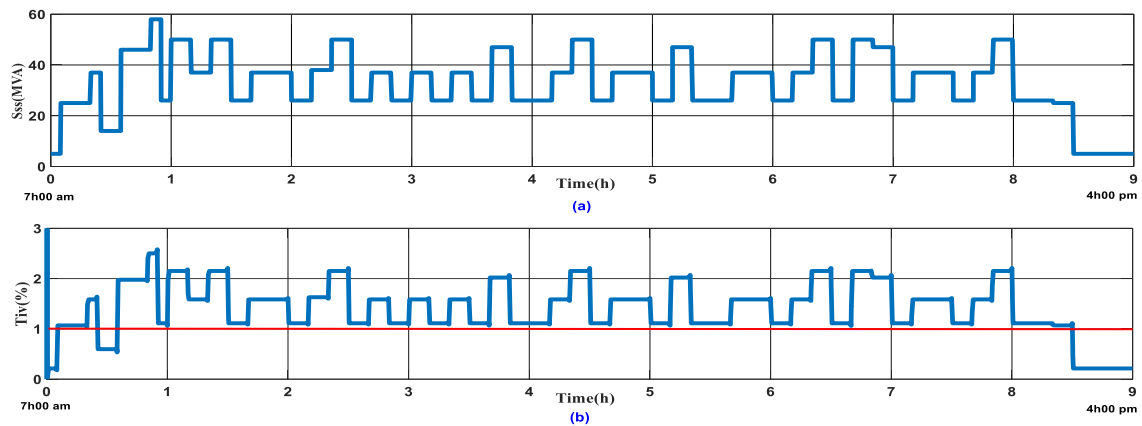
Figure 4. Evolution of (a) daily rail traffic for the Tangier substation (pk10) in 2030 (225 kV) and (b) predicted unbalance factor for the tangier substation (225 kV)

Figure 5 presents the evolution of different parameters (power consumed and unbalance factor) in degraded situation (N-1) for Tangier substation. Figure 5(a) present the power consumed. Figure 5(b) present the results of the voltage unbalance analysis.
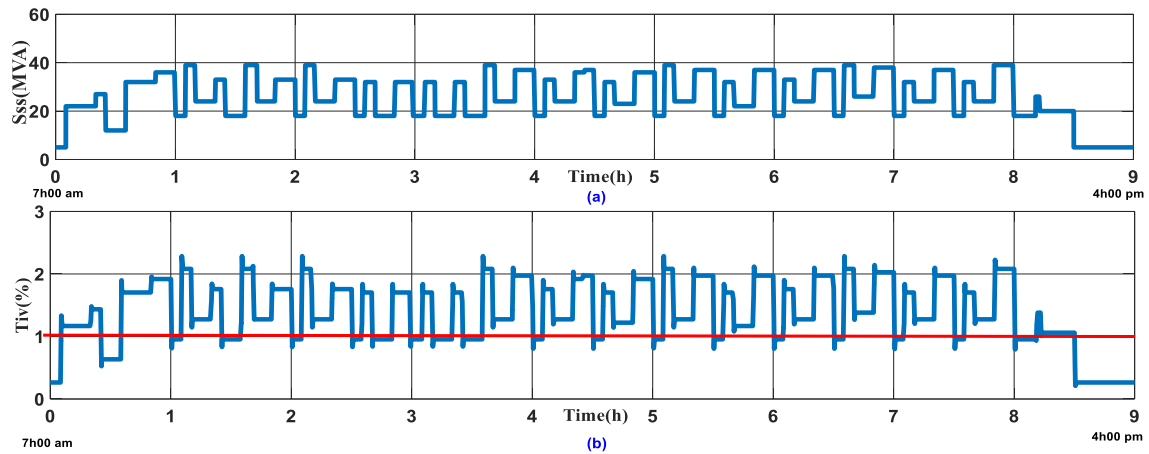

Figure 5. Evolution of (a) daily rail traffic for the tangier substation (pk10) in 2030 (202 kV) and (b) predicted unbalance factor for the tangier substation (202 kV)

Figure 6 presents the evolution of different parameters (power consumed and unbalance factor) in normal situation (N) for Kenitra substation, Figure 6(a) present the power consumed, and Figure 6(b) present the results of the voltage unbalance analysis. Figure 7 presents the evolution of different parameters (power consumed and unbalance factor) in degraded situation (N-1) for Kenitra substation, Figure 7(a) present the power consumed, and Figure 7(b) present the results of the voltage unbalance analysis.

In 2030, the unbalance factor for the both substations will exceed the limit value whatever the situation of the power grid (N or N-1), it can go up to 2.5%. This excess generates penalties on the energy consumed by the Moroccan railway operator (ONCF). For this reason, the railway operator (ONCF) project to install the unbalance compensators based on FACTS systems, which must be sized on the basis of the substation consumed power Sss (MVA).
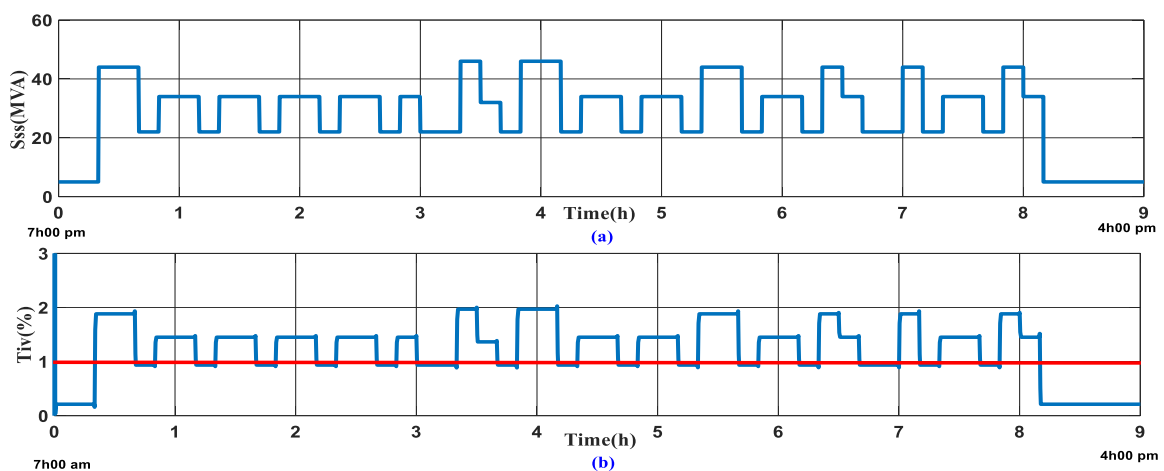

Figure 6. Evolution of (a) daily rail traffic for the Kenitra substation (pk185) in 2030 (225 kV) and (b) predicted unbalance factor for the Kenitra substation (225 kV)
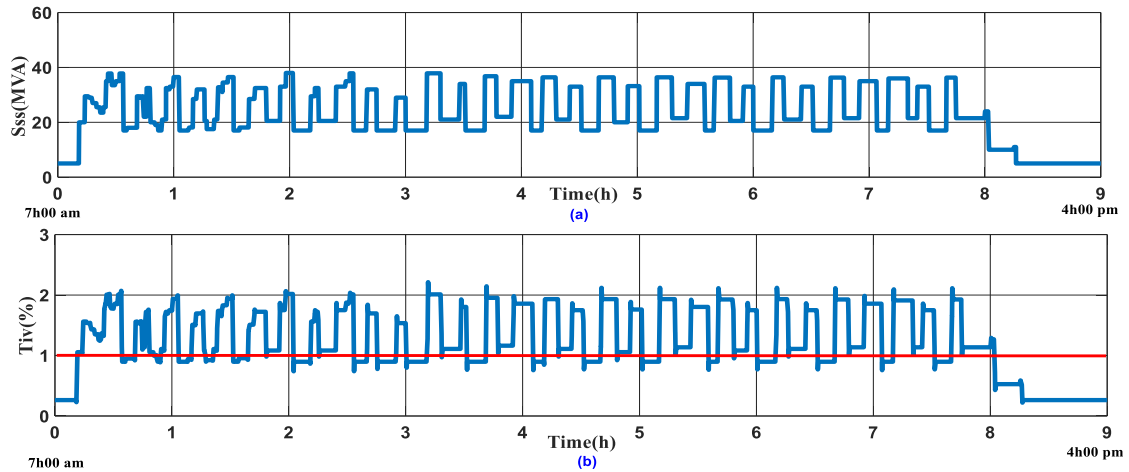
Figure 7. Evolution of (a) daily rail traffic for the Kenitra substation(pk185) in 2030 horizon (202 kV) and (b) predicted unbalance factor for the Kenitra substation in 2030 (202 kV)

3. CCI COMPENSATOR

3.1. Concept of the CCI

The Steinmetz circuit represents a common solution for balancing high power industrial single-phase loads. This technique consists of connecting an inductive and a capacitive impedance to the single-phase load in order to reduce the unbalance factor in the power supply system [15]-[19]. The disadvantage of the Steinmetz circuit is that it can only be used for static loads, so it is not more efficient for dynamic loads (railway substation), to adapt Steinmetz solution to our case, a dynamic capacitive and inductive impedance will be used depending on the power load. The realization of a variable impedance is possible with a PWM-controlled AC inverter as shown in Figure 8. The power structure of the CCI consists of two controlled impedances, one inductive and the other capacitive (Figure 9). Each impedance is supplied by a step-down transformer. An LC filter upstream of each impedance to limit the harmonic in the secondary of the transformer.
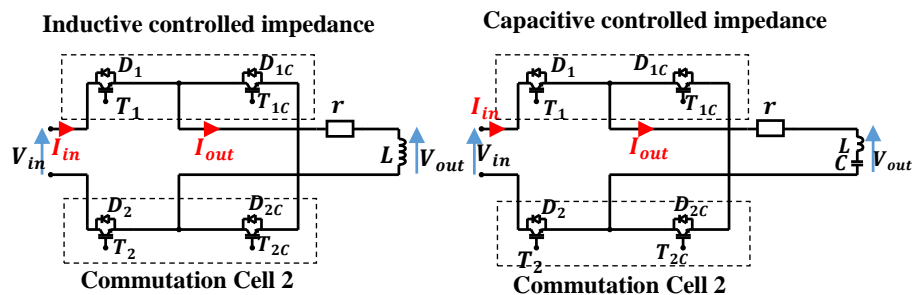

Figure 8. The inductive and capacitive variable impedances for CCI compensator

3.2. Sizing of the CCI compensator

Figure 10 shows the general structure of the CCI compensator, the set point impedance ($z_{in,c}$) is calculated from the power consumption S_{SS} using (1) and (2). The (3) explains the relationship to calculate the duty cycle alpha, which will later be a solicitation for the AC-chopper control in the form of PWM signals. LC filter is installed between the input part of the compensator and the transformer secondary in order to reduce THD.
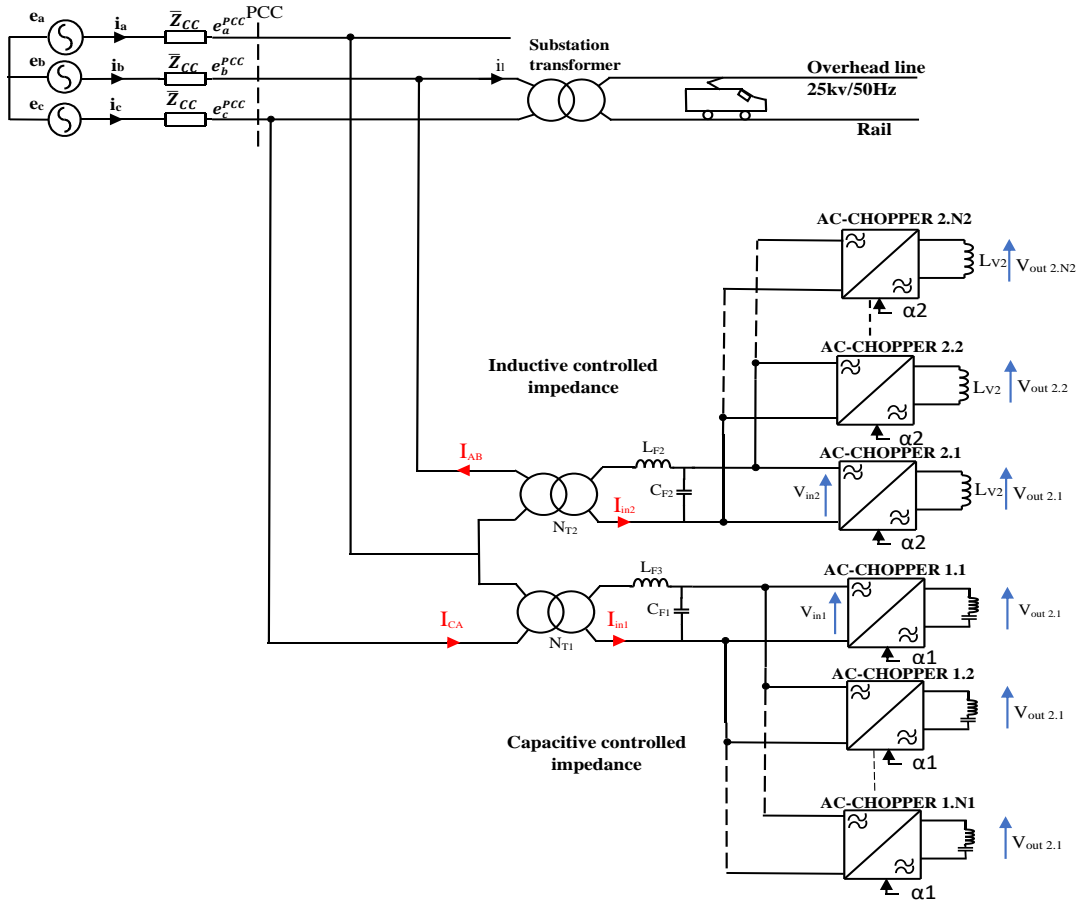
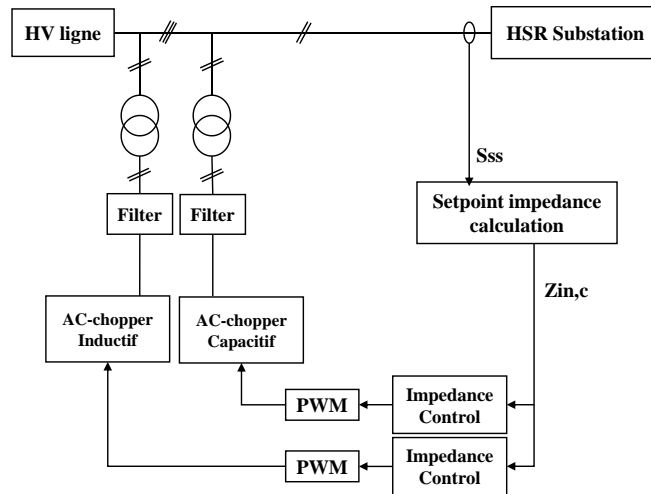Figure 9. Insertion of the active Steinmetz circuit in the substation

Figure 10. The general structure of the CCI compensator

3.2.1. IGBT module

The IGBTs module are chosen of ABB company. The technical specifications are satisfied for HV application. The maximum direct current at the thermal limit of the converter is 1.2 KA and a maximum reverse voltage is 4.5 kV.

3.2.2. Transformer

The role of the transformer is to step down the voltage in order to adapt it to the power electronic components used IGBT. The second role is a galvanic isolation because the compensator is connected directly to the high voltage (HV) electrical power transmission line. In this case the primary voltage of the transformer is 225 kV, and the secondary voltage is 3.5 kV, (3) the transformation ratio.

$$m_{T1} = m_{T2} = 15.55 \cdot 10^{-3} \tag{1}$$

3.2.3. Impedance variation range

From the power simulation provided by the ONCF, the range of power consumed by the substation varies between $R_{ss,min}$ and $R_{ss,min}$ (Table 2) and therefore deduce the extremities of the resistances $X_{L,max} = X_{C,max}$ and $X_{L,min} = X_{C,min}$ (2) and (3).

$$R_{ss} = \frac{U(V)^2}{S_{ss}(VA)} \tag{2}$$

Where U is the voltage of the high voltage line (225 kV), R_{SS} is the equivalent resistance of the sub-station, S_{SS} is the power consumed by the substation.

$$Z_C = Z_L = \sqrt{3}R_{ss} \tag{3}$$

Where Z_C is the capacitive impedance and Z_L is the inductive impedance.

Table 2. Primary impedance interval calculations

$S_{(ss,min)}$	5 MVA
$S_{(ss,max)}$	60 MVA
$R_{(ss,min)}$	10.125 KΩ
$R_{(ss,max)}$	0.843 KΩ
$X_{(L,max)} = X_{(C,max)}$	17.537 KΩ
$X_{(L,min)} = X_{(C,min)}$	1.461 KΩ

3.2.4. Duty cycle range

To determine the range of variation of the duty cycle alpha (α), if we assume that alpha=1 the impedance is $Z_C = Z_{c,min}$ and from (4) the minimum α is deduced. Table 3 shows the range of variation α as a function of impedance.

$$Z_{in} \approx \frac{Z_{out}}{\alpha^2} \tag{4}$$

Where Z_{in} is the input impedance and Z_{out} is the output impedance.

Table 3. Duty cycle interval calculations

$Z_{c,min}$	1.461 KΩ	α_{max}	1
$Z_{c,max}$	17.537 KΩ	α_{min}	0.288

3.2.5. Sizing of capacitive CCI

The reactive power produced by the capacitive CCI is calculated by (5), the results of the calculation of extreme values from α are presented in the Table 4, Table 5 presents the different parameters of CCI capacitive [20]-[22].

$$Q_C = \frac{U^2}{Z_{comp}} \tag{5}$$

Where Q_C is the reactive power of the compensator, Z_{com} is the impedance of the compensator. In order to supply the total reactive power produced by the capacitive CCI, the optimal number of cells of AC-chopper cells a PWM control is $N1 = 12$ cells in parallel.

Table 4. Reactive power range			
α_{max}	1	$Q_{c,max}(MVAR)$	34
α_{min}	0.273	$Q_{c,min}(MVAR)$	2.886

Table 5. The parameters of the capacitive compensator				
$X_{cv}(\Omega)$	$C_v(\mu F)$	$X_{Lcv}(\Omega)$	$L_{LC}(mH)$	$I_{max}(A)$
3.328	831	0.114	0.362	887.8

3.2.6. Sizing of inductive CCI

In the same way as for the capacitive CCI. The inductive limited impedance must consume a variable reactive power in the same range as the capacitive power. To compensate totally, 8 AC-chopper cells are needed, the Table 6 shows the calculation results for one cell.

Table 6. The parameters of the indicative compensator			
$X_L(\Omega)$	$L(mH)$	$r(m\Omega)$	$I_{max}(A)$
2.513	8	31.2	1050

3.2.7. LC filter sizing

The principal objective of the filter is to eliminate low frequency harmonics, but at the same time it should not influence the total impedance of the CCI. The variation range of the compensator impedance has been calculated $Z_{comp} = [Z_{min}; Z_{max}]$ In order that the filter impedance does not influence the total impedance of the compensator (Table 7), the following conditions must be respected:
- X_{CF} is maximum possible
- X_{LF} is minimum possible

The THD in voltage is controlled at a value 6.6% lower than the normalized limit (8% according to the NF EN 50160 Standard).

Table 7. The parameters of the indictive compensator	
L_F	C_F
92 µH	65.51 µF

4. RESULTS AND DISCUSSION

Figures 11-14 present the results obtained for the two situations (N and N-1) of the both substations (Tangier and Kenitra), the Figures show that the voltage unbalance factor (Tiv) and the voltage harmonic distortion factor (THDv) of CCI {CCI capacitive: THDc, CCI inductive: THDL} in function of the prediction of the daily rail traffic for the horizon 2030 are respecting the norms of the limits imposed by the energy provider (Tiv <1%).
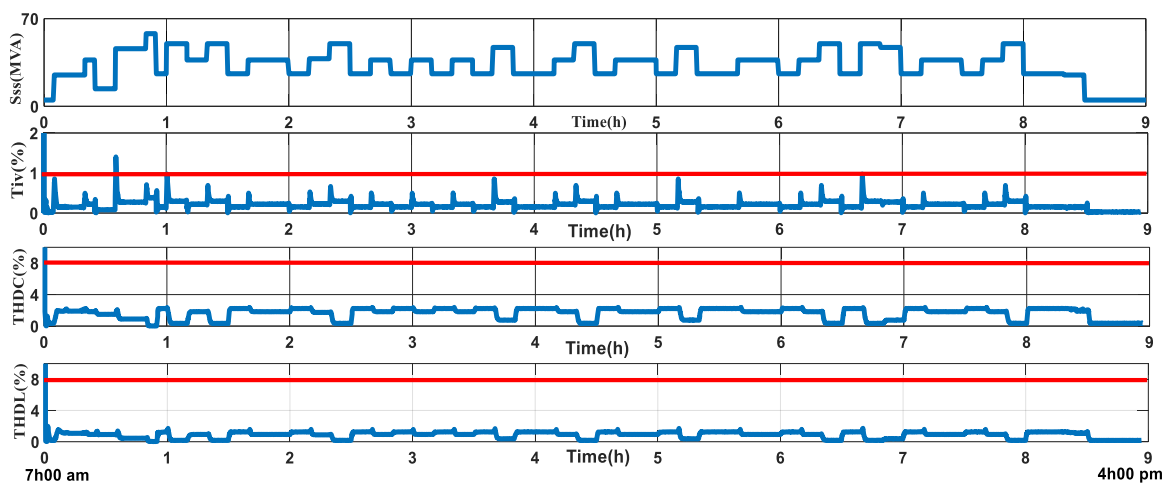

Figure 11. T_{iv} and THD according to daily railway traffic Tangier 225 kV with unbalance compensation by CCI (Cosφ ≈1)
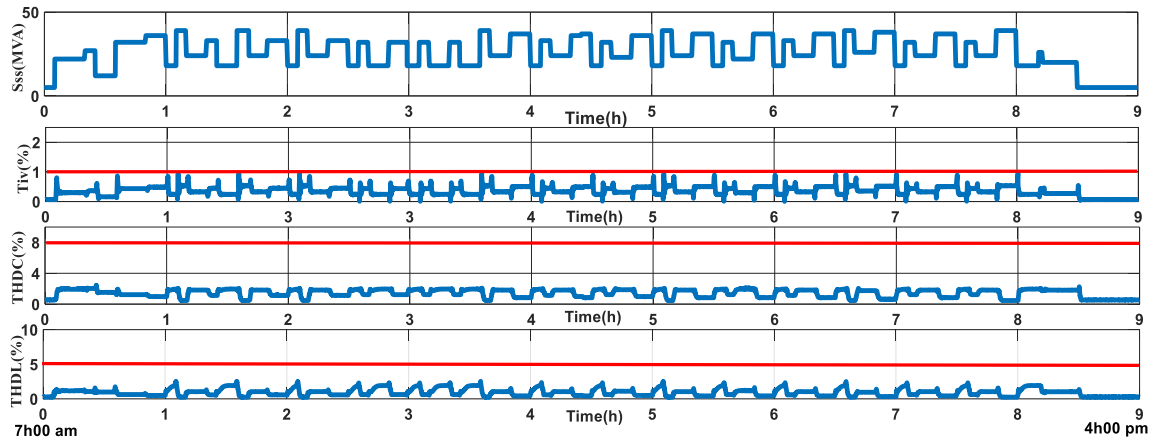
Figure 12. T_{iv} and THD according to daily railway traffic Tangier 202 kV with unbalance compensation by CCI (Cosφ ≈1)
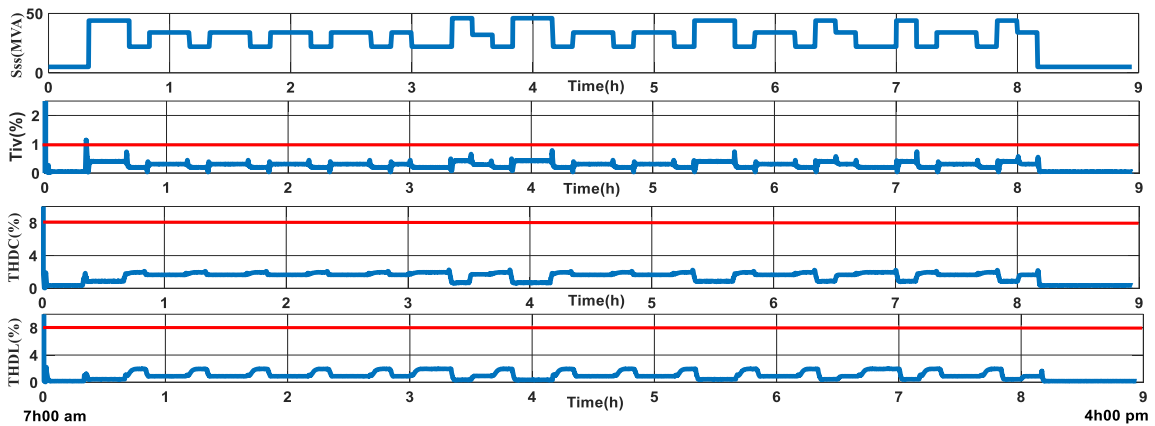

Figure 13. T_{iv} and THD based on daily railway traffic Kenitra 225 kV with unbalance compensation by CCI (Cosφ ≈1)
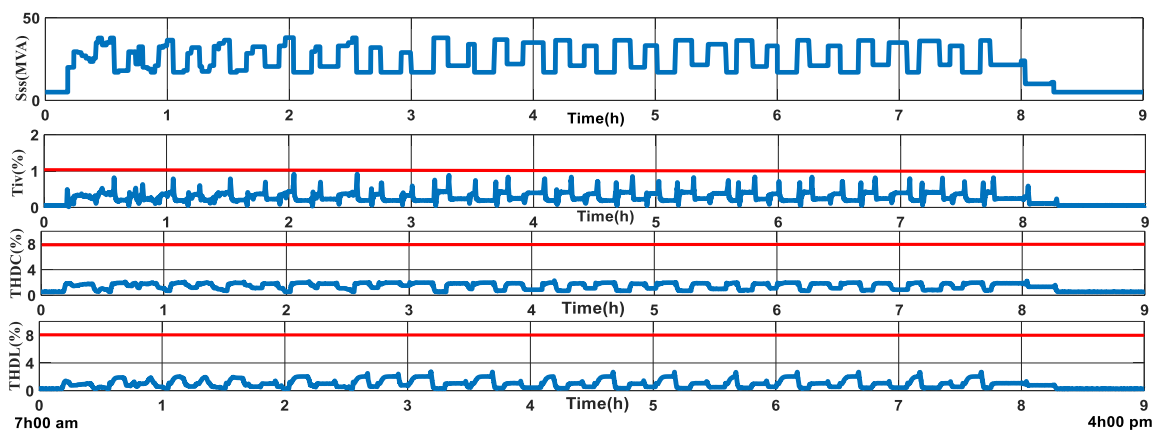

Figure 14. T_{iv} and THD based on daily railway traffic Kenitra 202 kV with unbalance compensation by CCI (Cosφ ≈1)

The variation of the power factor (cosphi of the substation) influences the quality of the unbalance compensation as shown in Figure 15 and Figure 16 for a power factor of 0.9 and 0.8 respectively of the

Tangier substation. From the simulation results, it is clear that the CCI compensator is able to compensate the unbalance for all loads with a power factor higher than 0.9 (Cosφ ≥0.9).
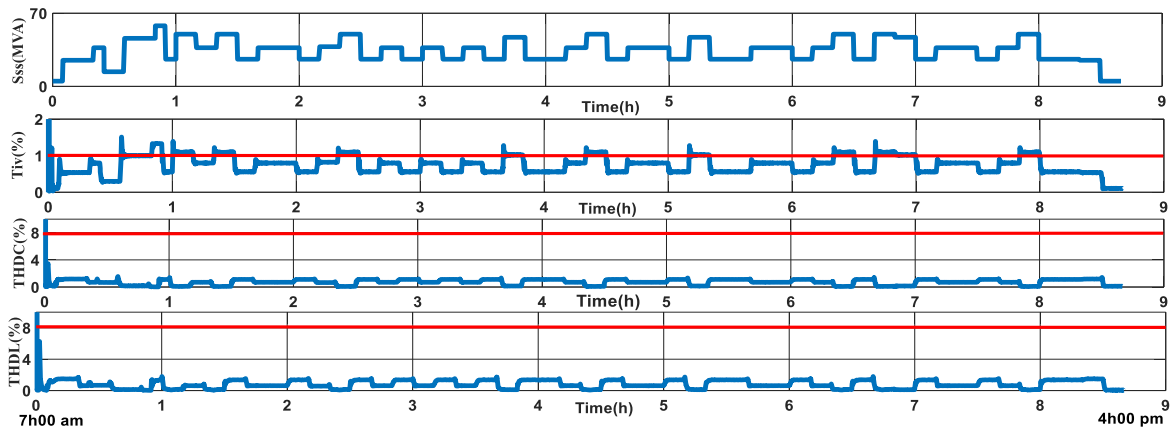

Figure 15. T_{iv} and THD according to daily railway traffic Tangier 225 kV, Cosφ=0.9 with compensation of unbalance by CCI
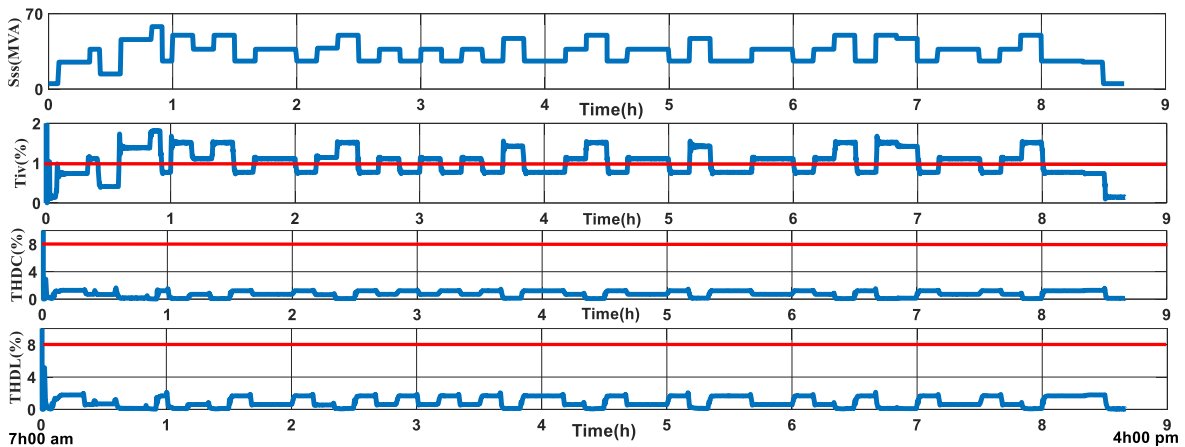

Figure 16. T_{iv} and THD according to daily railway traffic Tangier 225 kV, Cosφ=0.8 with unbalance compensation by CCI

Noting that the CCI compensator has proven its effectiveness in limiting the unbalance factor, it is also very important to see the losses generated by the semi-conductors constituting this compensator by comparing them with the existing compensators (VSI and CSI STATCOM). From the conduction and switching losses equations [23]-[25], it can be noticed that they depend on the values of the duty cycle α, which varies with the power consumed by the high-speed railway substation. To evaluate the efficiency of the CCI Table 8 presents the maximum power losses dissipated in the CCI compensator.

Table 8. The maximum power losses dissipated in the CCI compensator

maximum total losses (MW)		
CCI inductive	CCI capacitive	total
0, 29	0.17	0.46

The three topologies with their daily and annual consumption are represented in Table 9, noting that the CCI compensator has again proven its performance in terms of power losses in the semiconductors compared to the VSI and CSI STATCOM topologies [1].

Table 9. Semiconductor power losses for the three topologies CCI, VSI and CSI STATCOM

Unbalance compensator topology	Energy lost daily (MWh)	Energy lost annually (MWh)
CCI	2.8901	1054.89
VSI_STATCOM	44.46	16227.9
CSI_STATCOM	38.7	14125.5

The AC Chopper-based solution can be adopted by the Moroccan railway operator for the Tangier-Kenitra substations and has significant cost advantages over STATCOM solutions. The comparison between AC Chopper, VSI and CSI STATCOM topologies in terms of annual semiconductor losses has shown that our solution provides a very important reduction of power losses.

5. CONCLUSION

The increase in railway traffic poses the question of power quality in the substations of high-speed railway lines. In order to respect the exigencies imposed by the energy supplier (ONEE) and to guarantee a safe power quality, the railway operator is obliged to install unbalance compensators based on electronic power converters in the substations. This paper proposes a new compensation topology based on power electronics elements for 2×25 kV/50 Hz railway substations. The PWM AC-chopper controlled impedances are presented as converter structures characterized by reduced losses compared to STATCOM solutions. A comparative study between the proposed topology and the widely used STATCOM topology shows that power losses in semiconductors are about 92% lower. The experimental validation for this comparative study is the objective of a second paper.

REFERENCES

[1] A. Benslimane, J. Bouchnaif, M. Essoufi, B. Hajji, and L. el Idrissi, "Comparative study of semiconductor power losses between CSI-based STATCOM and VSI-based STATCOM, both used for unbalance compensation," *Protection and Control of Modern Power Systems*, vol. 5, no. 1, Feb. 2020, doi: 10.1186/s41601-019-0150-4.

[2] H. Y. Kuo and T. H. Chen, "Rigorous evaluation of the voltage unbalance due to high-speed railway demands," *IEEE Transactions on Vehicular Technology*, vol. 47, no. 4, pp. 1385–1389, 1998, doi: 10.1109/25.728533.

[3] Q. Y. Liu, X. R. Li, X. J. Li, B. Lei, D. S. Chen, and Y. Pan, "Impact of negative sequence current of traction load on the grid running state," in *APAP 2011 - Proceedings: 2011 International Conference on Advanced Power System Automation and Protection*, Oct. 2011, vol. 2, pp. 879–883, doi: 10.1109/APAP.2011.6180535.

[4] A. Von Jouanne and B. Banerjee, "Assessment of voltage unbalance," *IEEE Transactions on Power Delivery*, vol. 16, no. 4, pp. 782–790, 2001, doi: 10.1109/61.956770.

[5] S. K. Mishra and L. N. Tripathy, "A critical fault detection analysis & fault time in a UPFC transmission line," *Protection and Control of Modern Power Systems*, vol. 4, no. 1, Feb. 2019, doi: 10.1186/s41601-019-0117-5.

[6] L. Yiqiao and C. O. Nwankpa, "A new type of STATCOM based on cascading voltage-source inverters with phase-shifted unipolar SPWM." *IEEE transactions on industry applications* 35, no. 5, pp. 1118-11235, 1999, doi: 10.1109/28.793373.

[7] A. Benslimane, J. Bouchnaif, M. Azizi, and K. Grari, "Study of a STATCOM used for unbalanced current compensation caused by a high speed railway (HSR) sub-station," in *Proceedings of 2013 International Renewable and Sustainable Energy Conference, IRSEC 2013*, Mar. 2013, pp. 441–446, doi: 10.1109/IRSEC.2013.6529724.

[8] R. Omar and N. A. Rahim, "Voltage unbalanced compensation using dynamic voltage restorer based on supercapacitor," *International Journal of Electrical Power and Energy Systems*, vol. 43, no. 1, pp. 573–581, Dec. 2012, doi: 10.1016/j.ijepes.2012.05.015.

[9] Z. Li, W. Li, and T. Pan, "An optimized compensation strategy of DVR for micro-grid voltage sag," *Protection and Control of Modern Power Systems*, vol. 1, no. 1, Jul. 2016, doi: 10.1186/s41601-016-0018-9.

[10] S. K. Routray, N. Nayak, and P. K. Rout, "A robust fuzzy sliding mode control design for current source inverter based STATCOM application," *Procedia Technology*, vol. 4, pp. 342–349, 2012, doi: 10.1016/j.protcy.2012.05.052.

[11] A. Ghorbani, S. Y. Ebrahimi, and M. Ghorbani, "Active power based distance protection scheme in the presence of series compensators," *Protection and Control of Modern Power Systems*, vol. 2, no. 1, Mar. 2017, doi: 10.1186/s41601-017-0034-4.

[12] D. Shen and P. W. Lehn, "Modeling analysis and control of a current source inverter-based STATCOM," *IEEE Power Engineering Review*, vol. 21, no. 11, pp. 61–61, Nov. 2008, doi: 10.1109/mper.2001.4311174.

[13] A. Benslimane, J. Bouchnaif, M. Azizi, and K. Grari, "State feedback controller for current source inverter Based STATCOM used for unbalance compensation in high voltage power grid," in *Proceedings of 2014 International Renewable and Sustainable Energy Conference, IRSEC 2014*, Oct. 2014, pp. 861–865, doi: 10.1109/IRSEC.2014.7059757.

[14] M. Benzaouia, B. Hajji, A. Rabhi, A. Mellit, A. Benslimane, and A. M. Dubois, "Energy management strategy for an optimum control of a standalone photovoltaic-batteries water pumping system for agriculture applications," in *Lecture Notes in Electrical Engineering*, vol. 681, Springer Singapore, 2021, pp. 855–868.

[15] P. Ladoux, A. Lowinsky, P. Marino, and G. Raimondo, "Reactive power compensation in railways using active impedance concept," in *SPEEDAM 2010 - International Symposium on Power Electronics, Electrical Drives, Automation and Motion*, Jun. 2010, pp. 1362–1367, doi: 10.1109/SPEEDAM.2010.5542106.

[16] R. Rakhmawati and F. D. Murdianto, "AC-AC voltage controller of power supply for heater on drying system," *Telkomnika (Telecommunication Computing Electronics and Control)*, vol. 16, no. 3, pp. 1061–1070, Jun. 2018, doi: 10.12928/TELKOMNIKA.v16i3.5194.

[17] P. Ladoux, G. Raimondo, H. Caron, and P. Marino, "Chopper-controlled steinmetz circuit for voltage balancing in railway substations," *IEEE Transactions on Power Electronics*, vol. 28, no. 12, pp. 5813–5822, Dec. 2013, doi: 10.1109/TPEL.2013.2242492.

[18] P. Ladoux, J. Fabre, and H. Caron, "Power quality improvement in ac railway substations: The concept of chopper-controlled impedance," *IEEE Electrification Magazine*, vol. 2, no. 3, pp. 6–15, Sep. 2014, doi: 10.1109/MELE.2014.2331792.

[19] A. S. Hussein and M. N. Hawas, "Power quality analysis based on simulation and MATLAB/Simulink," *Indonesian Journal of Electrical Engineering and Computer Science*, vol. 16, no. 3, pp. 1144–1153, Dec. 2019, doi: 10.11591/ijeecs.v16.i3.pp1144-1153.

[20] T. Furuhashi, S. Okuma, and Y. Uchikawa, "A Study on the Theory of Instantaneous Reactive Power," *IEEE Transactions on Industrial Electronics*, vol. 37, no. 1, pp. 86–90, 1990, doi: 10.1109/41.45848.

[21] A. B. Mohammed, M. A. M. Ariff, and S. N. Ramli, "Power quality improvement using dynamic voltage restorer in electrical distribution system: An overview," *Indonesian Journal of Electrical Engineering and Computer Science*, vol. 17, no. 1, pp. 86–93, Jan. 2019, doi: 10.11591/ijeecs.v17.i1.pp86-93.

[22] W. Hofmann, J. Schlabbach, and W. Just, *Reactive Power Compensation: A Practical Guide*. Wiley, 2012.

[23] M. H. Bierhoff and F. W. Fuchs, "Semiconductor losses in voltage source and current source IGBT converters based on analytical derivation," in *PESC Record - IEEE Annual Power Electronics Specialists Conference*, 2004, vol. 4, pp. 2836–2842, doi: 10.1109/PESC.2004.1355283.

[24] K. Berringer, J. Marvin, and P. Perruchoud, "Semiconductor power losses in AC inverters," in *Conference Record - IAS Annual Meeting (IEEE Industry Applications Society)*, 1995, vol. 1, pp. 882–888, doi: 10.1109/ias.1995.530391.

[25] S. Z. Ahmed, M. N. Tandjaoui, M. Djebbar, C. Benachaiba, and B. Mazari, "Power quality enhancement by using D-FACTS systems applied to distributed generation," *International Journal of Power Electronics and Drive Systems (IJPEDS)*, vol. 10, no. 1, p. 330, Mar. 2019, doi: 10.11591/ijpeds.v10.i1.pp330-341.

BIOGRAPHIES OF AUTHORS

Ismail Mir received the degree of Electrical and Electronic Engineer from National school of applied science, Mohammed First University, Oujda, Morocco in 2020. His main study is on control strategies in the power grid and FACTS system. He is currently pursuing a PhD in Electrical Engineering in the same school and university. He can be contacted at email: ismail.mir@ump.ac.ma.

Prof. Dr. Anas Benslimane is associate professor at National school of applied science, Mohammed first university, Oujda, Morocco. He received the State engineer's degree in industrial engineering from National school of applied science Oujda. He holds the Phd degrees in electrical engineering from Mohammed First University. His research areas are FACTS devices and power grids, he is a reviewer in some conferences. He can be contacted at email: a.benslimane@ump.ac.ma.

Prof. Dr. Jamal Bouchnaif is associate professor at High Institute of Technology, Mohammed first university, Oujda, Morocco. He received the Bachelor degree in electrical engineering from high national school of technical studies Rabat. He holds the Master's and Phd degrees in electrical engineering from Mohammed First University. His research areas are electrical drives and grids, noise, vibration and iron losses of switched reluctance motor. He holds many international certifications, NC3, Snapon. And also, some conference prices. He is the chairman of the international conference of mechanical industrial energy systems and automotive technology ICMIESAT. He is cofounder of mechatronic center and innovation and prototyping center of the Mohammed First University Oujda. He is a director of electrical engineering and maintenance laboratory Oujda. He can be contacted at email: j.bouchnaif@ump.ac.ma.

Prof. Dr. Badreddine Lahfaoui his expertise in control systems, System identification and control, power electronics, renewable energies, wind turbine, PV systems, Hybrid systems, control cards. His focus is based on the use of controller systems to have application in Engineering field. He was warded his PhD in electrical engineering from the Mohamed First University, Oujda, Morocco. He published more than 8 papers. His H-index is 5 on Scopus. He can be contacted at email: b.lahfaoui@ump.ac.ma.